Korean Journal of Radiology

High-Resolution Magnetic Resonance Imaging Using Compressed Sensing for Intracranial and Extracranial Arteries: Comparison with Conventional Parallel Imaging

Chong Hyun Suh, MD, Seung Chai Jung, MD, PhD, Ho Beom Lee, RT, Se Jin Cho, MD

All authors: Department of Radiology and Research Institute of Radiology, University of Ulsan College of Medicine, Asan Medical Center, Seoul, Korea

Objective: To compare conventional sensitivity encoding (SENSE) to compressed sensing plus SENSE (CS) for high-resolution magnetic resonance imaging (HR-MRI) of intracranial and extracranial arteries.

Materials and Methods: HR-MRI was performed in 14 healthy volunteers. Three-dimensional T1-weighted imaging (T1WI) and proton density-weighted imaging (PD) were acquired using CS or SENSE under the same total acceleration factors (AF_t)–5.5, 6.8, and 9.7 for T1WI and 3.2, 4.0, and 5.8 for PD–to achieve reduced scanning times in comparison with the original imaging sequence (SENSE T1WI, AF_t 3.5; SENSE PD, AF_t 2.0) using the 3-tesla system. Two neuroradiologists measured signal-to-noise ratio (SNR) and contrast-to-noise ratio (CNR), and used visual scoring systems to assess image quality. Acceptable imaging was defined as a visual score $\geq$ 2. Repeated measures analysis of variance and Cochran's Q test were performed.

Results: CS yielded better image quality and vessel delineation than SENSE in T1WI with AF_t of 5.5, 6.8, and 9.7, and in PD with AF_t of 5.8 ($p < 0.05$). CS T1WI with AF_t of 5.5 and CS PD with AF_t of 3.2 and 4.0 did not differ significantly from original imaging ($p > 0.05$). SNR and CNR in CS were higher than they were in SENSE, but lower than they were in the original images ($p < 0.05$). CS yielded higher proportions of acceptable imaging than SENSE (CS T1WI with AF_t of 6.8 and PD with AF_t of 5.8; $p < 0.0167$).

Conclusion: CS is superior to SENSE, and may be a reliable acceleration method for vessel HR-MRI using AF_t of 5.5 for T1WI, and 3.2 and 4.0 for PD.

Keywords: *Intracranial artery disease; Image quality; Undersampling; Reconstruction method; Signal-to-noise ratio; Contrast-to-noise ratio; Compressed sensing*

INTRODUCTION

With its high spatial resolution and excellent soft-tissue

Corresponding author: Seung Chai Jung, MD, PhD, Department of Radiology and Research Institute of Radiology, University of Ulsan College of Medicine, Asan Medical Center, 88 Olympic-ro 43-gil, Songpa-gu, Seoul 05505, Korea.
• Tel: (822) 3010-3949 • Fax: (822) 476-4719
• E-mail: dynamics79@gmail.com

contrast, high-resolution magnetic resonance imaging (HR-MRI) for the visualization of vessel walls and contours is of substantial interest (1). Intracranial vessel wall MRI is a useful adjunct to digital subtraction angiography for differentiating intracranial artery disease and identifying symptomatic non-stenotic disease (1-4). However, the long imaging acquisition time of HR-MRI of the vessel wall is an important issue in daily clinical practice. A long acquisition time can lead to degradation of image quality due to the higher probability of motion artifacts, especially in elderly patients or those who have recently had a stroke. Conventional parallel imaging techniques such as sensitivity encoding (SENSE) or generalized auto-calibrating partial parallel acquisition have been developed (5, 6); however, they can adversely affect image quality and the visualization of target diseases. Although a two-

dimensional spatially selective radiofrequency excitation pulse can achieve an acceptable reduction in scan time, this may be achieved at the cost of limited scan coverage (2). Therefore, a novel sequence for vessel HR-MRI is required, to reduce image acquisition time while maintaining image quality and vessel delineation.

Lustig et al. (7) developed compressed sensing for rapid MRI, and demonstrated accelerated acquisition times and improved spatial resolution in multi-slice fast spin echo brain imaging and three-dimensional (3D) contrast-enhanced angiography. Compressed sensing enables accelerated MRI by using wavelet transformations and nonlinear iterative reconstruction from variable-density random undersampling of k-space data (7). Conventional parallel imaging techniques also reduce scanning time by undersampling, but the undersampling is done uniformly and images are reconstructed using surface coil information. Different undersampling and reconstruction methods may have different influences on image quality and spatial resolution. Previous studies suggest that compressed sensing can be successfully applied to vessel MRI for intracranial and extracranial arteries, resulting in reduced image acquisition time while maintaining image quality and vessel wall delineation (8, 9). To our knowledge however, to date no study investigating the application of compressed sensing to intracranial vessel HR-MRI and evaluating compressed sensing in comparison with conventional parallel imaging (SENSE) has been reported.

The aim of the current study was to compare SENSE with compressed sensing plus SENSE (CS) for HR-MRI of intracranial and extracranial arteries, including the evaluation of a number of different acceleration factors.

MATERIALS AND METHODS

The relevant Institutional Review Board approved this study, and informed consent was obtained from all subjects.

Study Population

Fourteen healthy volunteers underwent HR-MRI for delineation of intracranial and extracranial arteries between September 2017 and November 2017. Of these 14 patients, 7 were men (mean age, 58.6 years; age range, 40–67 years) and 7 were women (mean age, 55.3 years; age range, 33–65 years), and the overall mean age was 56.9 years (age range, 33–67 years).

Image Acquisition

All MRI examinations were performed using a 3T system (Ingenia CX; Philips Medical Systems, Best, the Netherlands) with a 32-channel head coil, and 3D T1-weighted imaging (T1WI) and proton density-weighted imaging (PD) were acquired. CS is a newly developed technique combining compressed sensing and SENSE. For comparison purposes, T1WI with CS and SENSE (total acceleration factors [AF_t] 5.5, 6.8, and 9.7), and PD with CS and SENSE (AF_t 3.2, 4.0, and 5.8) were also acquired to achieve reduced scanning times in comparison with the original imaging sequence (SENSE T1WI with AF_t 3.5 and SENSE PD with AF_t 2.0). For the T1WI, compressed sensing factors of 1.6, 2.0, and 2.9 resulted in the CS T1WI having respective AF_t values of 5.5, 6.8, and 9.7. For the PD, compressed sensing factors of 1.6, 2.0, and 2.9 resulted in the CS PD having respective AF_t values of 3.2, 4.0, and 5.8. The imaging parameters for the original T1WI were echo time 15 ms, repetition time 900 ms, flip angle 90°, matrix 320 x 320 x 333, field of view 192 x 192 x 200 mm, voxel size 0.6 x 0.6 x 0.6 mm, acceleration factor 3.5, and acquisition time 9 minutes 18 seconds. The imaging parameters for the original PD were echo time 35 ms, repetition time 2000 ms, flip angle 90°, matrix 300 x 300 x 75, field of view 120 x 120 x 30 mm, voxel size 0.4 x 0.4 x 0.4 mm, acceleration factor 2, and acquisition time 12 minutes 36 seconds.

The total acquisition times for the T1WI were 9 minutes 18 seconds for the original sequence, 5 minutes 46 seconds (62% of the original scanning time) for CS and SENSE with AF_t 5.5, 4 minutes 39 seconds (50% of the original scanning time) for CS and SENSE with AF_t 6.8, and 3 minutes 15 seconds (35% of the original scanning time) for CS and SENSE with AF_t 9.7. The total acquisition times for the PD were 12 minutes 36 seconds for the original sequence, 7 minutes 52 seconds (62% of the original scanning time) for CS and SENSE with AF_t 3.2, 6 minutes 18 seconds (50% of the original scanning time) for CS and SENSE with AF_t 4.0, and 4 minutes 22 seconds (35% of the original scanning time) for CS and SENSE with AF_t 5.8.

Image Analysis

Two neuroradiologists who were blinded to the sequence information, one with 1 year of experience and the other with 7 years of experience independently assessed the images both qualitatively and quantitatively. In qualitative analyses, each T1WI acquisition was rated using a 4-point visual scoring system for image quality and vessel wall

delineation (10). Overall image quality and artifact were graded as follows: 0, poor image quality with large artifact; 1, moderate image quality with moderate artifact; 2, good image quality with slight artifact; 3, excellent image quality without artifact (Fig. 1). Vessel wall delineation was graded as follows: 0, less than 50% of the vessel wall is visible; 1, more than 50% of the vessel wall is visible; 2, the vessel wall is delineated with adequate signal and contrast to the lumen and cerebrospinal fluid (CSF); 3, the vessel wall is delineated with excellent signal and sharp contrast to the lumen and CSF (10). Each PD acquisition was rated for image quality using the same scoring system as for the T1WI, and vessel delineation of the outer contour and branching arteries were graded as follows: 0, less than 50% of the vessel is visible; 1, more than 50% of the vessel is

visible; 2, the vessel is delineated with adequate signal and contrast to the lumen and CSF; 3, the vessel is delineated with excellent signal and sharp contrast to the lumen and CSF (Fig. 2). Acceptable images were defined as those with scores ≥ 2 for both image quality and vessel delineation.

In quantitative analyses, signal-to-noise ratio (SNR) and contrast-to-noise ratio (CNR) measurements were obtained for the middle cerebral artery, basilar artery, terminal internal carotid artery, and carotid bulb. Digital Imaging and Communications in Medicine data derived from the magnetic resonance images were loaded into the "AsanJ" software developed in-house, which is based on a plug-in package for ImageJ (Bethesda, MD, USA; http://rsbweb.nih.gov/ij/) for lesion segmentation. The regions of interest (ROIs) used in the analysis were drawn by two
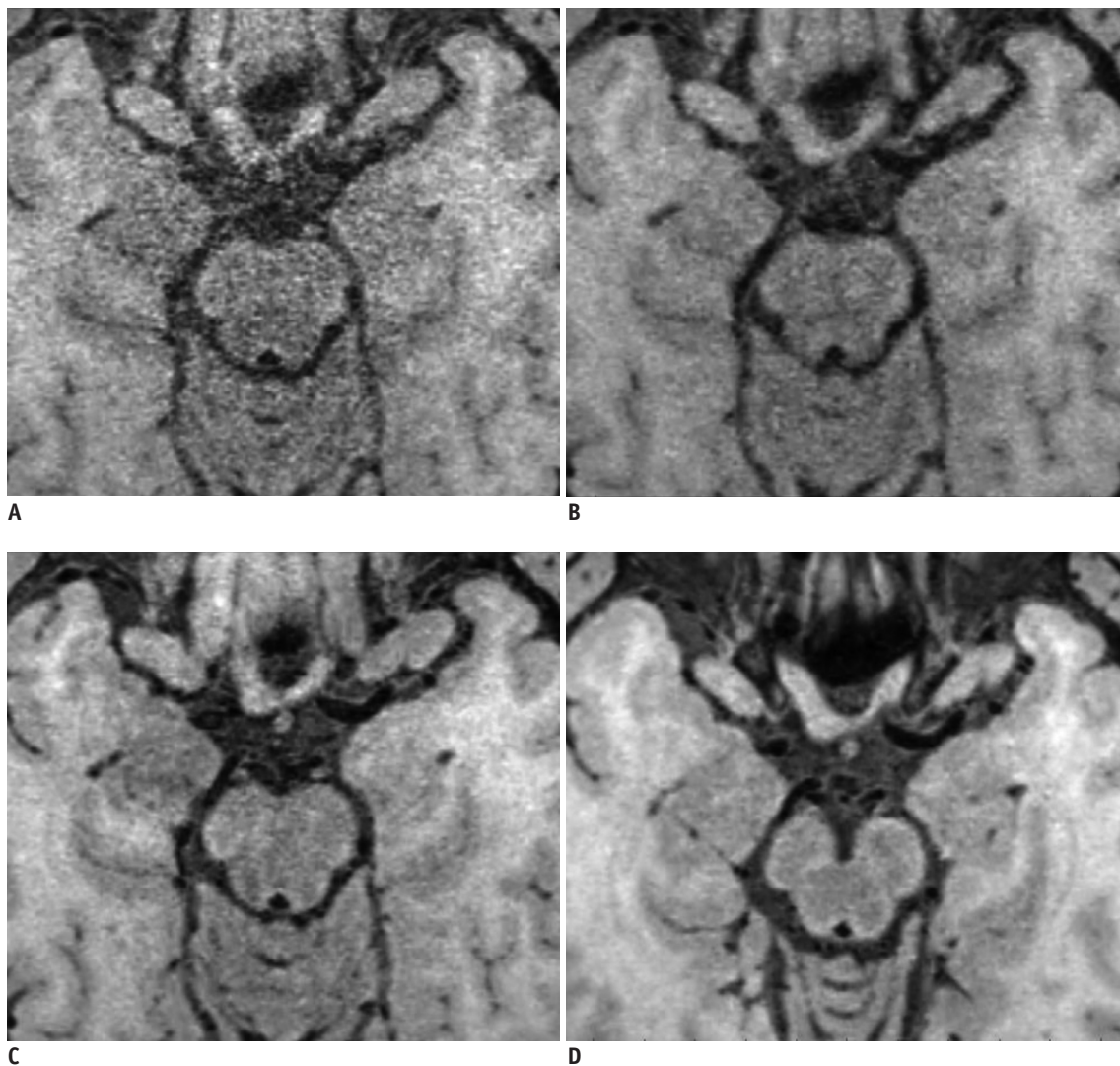

Fig. 1. Overall image quality and artifact were graded as follows.
(A) Grade 0, poor image quality with large artifact, **(B)** grade 1, moderate image quality with moderate artifact, **(C)** grade 2, good image quality with slight artifact, and **(D)** grade 3, excellent image quality without artifact.
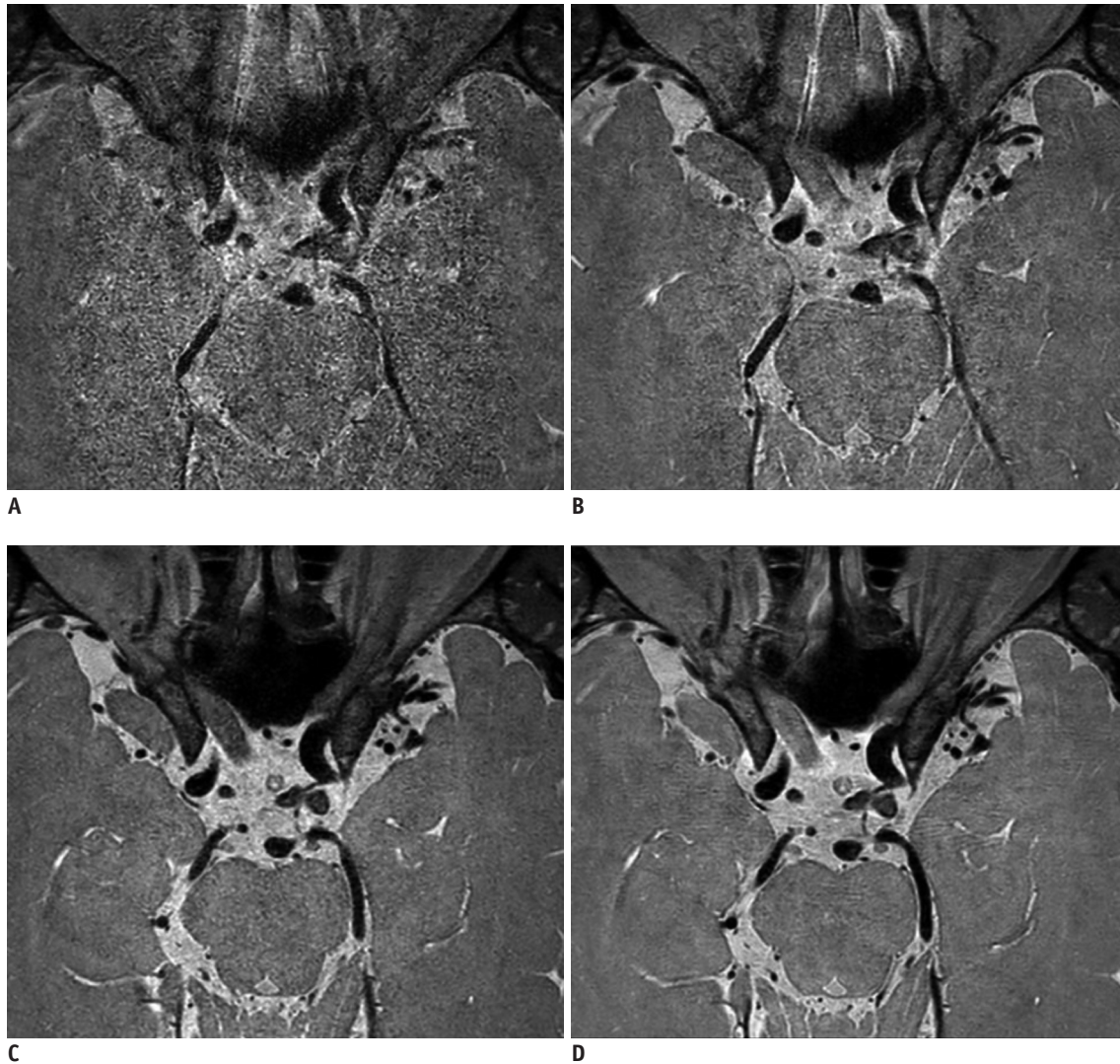
Fig. 2. Vessel delineations of outer contour and branching arteries were graded as follows.
(A) Grade 0, less than 50% of vessel is visible, **(B)** grade 1, more than 50% of vessel is visible, **(C)** grade 2, vessel is delineated with adequate signal and contrast to lumen and CSF, and **(D)** grade 3, vessel is delineated with excellent signal and sharp contrast to lumen and CSF. CSF = cerebrospinal fluid

neuroradiologists. An amplitude segmentation technique based on histogram features and the following formula was used to automatically place the ROIs (11, 12):

$$r_{i,j} = \begin{cases} 1, & T_{min} < p_{i,j} \leq T_{max} \\ 0, & \text{otherwise} \end{cases}$$

where $r_{i,j}$ is the resulting pixel at coordinate (i,j), $p_{i,j}$ is the corresponding pixel in the input image, and T is the threshold value. When the user places an initial region contour around a vessel wall and double-clicks the mouse, the software automatically calculates the threshold (T_{min}, T_{max}), and delineates the vessel wall to quantify its SNR. SNR_{wall}, SNR_{lumen}, and SNR_{CSF} for T1WI, and SNR_{wall} and SNR_{CSF} for PD were calculated as follows: SNR = 0.695 x (signal

intensity) / (noise), with noise measured as the standard deviation (SD) of the white matter signal (ROI area > 200 mm^2). Due to the inhomogeneous noise distribution as a result of parallel imaging, we could not directly measure the noise simply in the air. Instead, we used the SD of the white matter (13, 14). $CNR_{wall-lumen}$ and $CNR_{wall-CSF}$ for T1WI, and $CNR_{CSF-wall}$ for PD were calculated via the following formula (10):

$$CNR_{A-B} = SNR_A - SNR_B$$

Statistical Analysis

We combined the data-sets from both readers and performed all the analyses. For comparisons between

original, CS, and SENSE images, the Kolmogorov-Smirnov test was used to determine whether the continuous variables were normally distributed. Based on the results of the Kolmogorov-Smirnov test, repeated measures analysis of variance or Friedman tests were used to compare the visual scoring systems, SNR, and CNR of the original, CS, and SENSE images for both intracranial and extracranial arteries. Cochran's Q test was used to compare the proportions of acceptable images of each sequence. Post-hoc tests were performed using Bonferroni correction. We also compared acceptability, SNR, and CNR on T1WI for intracranial and extracranial arteries. Interobserver agreements for the original, CS, and SENSE images were assessed using intraclass correlation coefficients (ICCs) and weighted kappa. Two-way random models and consistency assumptions were used for ICC (15). The strength of interobserver agreement was categorized according to the ICC and weighted kappa values as follows: < 0.20, poor; 0.21–0.40, fair; 0.41–0.60, moderate; 0.61–0.80, good; 0.81–1.00, excellent (16). All statistical analyses were performed using SPSS software (version 20; IBM Corp., Armonk, NY, USA).

RESULTS

Qualitative Analysis

For T1WI, CS provided significantly better image quality and vessel wall delineation than SENSE across all AF_t values ($p < 0.05$). There was no significant difference between the CS sequence with AF_t 5.5 and the original sequence ($p > 0.05$) (Table 1). CS with AF_t 6.8 yielded higher proportions of acceptable imaging than SENSE with AF_t 6.8 ($p < 0.0167$). CS with AF_t 5.5 and 6.8 and SENSE with AF_t 5.5 yielded proportions of acceptable imaging that were similar to those of the original sequence ($p > 0.05$) (Table 2). Representative T1WI images are shown in Figure 3.

In PD, CS was significantly superior to SENSE with regard to image quality and vessel delineation for outer contour and branching arteries at AF_t 5.8 ($p < 0.05$). There were no statistically significant differences between the original image, CS with AF_t 3.2 and 4.0, and SENSE with AF_t 3.2 and 4.0 ($p > 0.05$) (Table 1). At an AF_t of 5.8, CS yielded higher proportions of acceptable imaging than SENSE ($p < 0.0167$). CS with AF_t 3.2, 4.0, and 5.8, and SENSE with AF_t 3.2 and 4.0 yielded proportions of acceptable imaging that were similar

Table 1. Comparisons of Visual Scoring Systems on HR-MRI T1WI and PD between Original, CS, and SENSE Imaging

	Acceleration Factor	Original (95% CI)	CS (95% CI)	SENSE (95% CI)	P
T1WI					
Image quality	Original	2.75 (2.55–2.95)			
	5.5		2.75 (2.58–2.92)	2.10 (1.99–2.23)	< 0.001[†‡]
	6.8		2.18 (1.99–2.36)	1.71 (1.51–1.92)	< 0.001[*†‡]
	9.7		1.32 (1.14–1.51)	0.46 (0.27–0.66)	< 0.001[*†‡]
Vessel wall delineation	Original	2.86 (2.72–3.00)			
	5.5		2.82 (2.67–2.97)	2.21 (2.05–2.38)	< 0.001[†‡]
	6.8		2.25 (2.08–2.42)	1.96 (1.77–2.16)	< 0.001[*†‡]
	9.7		1.07 (0.79–1.35)	0.39 (0.20–0.59)	< 0.001[*†‡]
PD					
Image quality	Original	2.96 (2.89–3.04)			
	3.2		2.96 (2.89–3.04)	2.82 (2.64–3.01)	0.182
	4.0		2.86 (2.65–3.06)	2.86 (2.72–3.00)	0.432
	5.8		2.54 (2.31–2.76)	1.82 (1.56–2.08)	< 0.001[*†‡]
Vessel outer contour/ branching arteries depiction	Original	2.93 (2.83–3.03)			
	3.2		2.93 (2.83–3.03)	2.71 (2.48–2.95)	0.089
	4.0		2.79 (2.57–3.01)	2.61 (2.39–2.83)	0.074
	5.8		2.04 (1.79–2.28)	1.21 (0.99–1.43)	< 0.001[*†‡]

When statistically significant differences were demonstrated by post-hoc tests using Bonferroni correction (Bonferroni corrected p value < 0.05), symbols (*, †, ‡) signify p values between original and CS (*), original and SENSE (†), and CS and SENSE (‡). CI = confidence interval, CS = compressed sensing plus SENSE, HR-MRI = high-resolution magnetic resonance imaging, PD = proton density-weighted imaging, SENSE = sensitivity encoding, T1WI = T1-weighted imaging

Table 2. Comparisons of Acceptable T1WI and PD HR-MRI between Original, CS, and SENSE Imaging

	Acceleration Factor	Original (95% CI)	CS (95% CI)	SENSE (95% CI)	P
Intracranial T1WI	Original	96.4 (81.7–99.9)			
	5.5		100 (87.7–100)	100 (87.7–100)	0.368
	6.8		96.4 (81.7–99.9)	64.3 (44.1–81.4)	< 0.001[†‡]
	9.7		21.4 (8.3–41.0)	0 (0–12.3)	< 0.001*[†]
Extracranial T1WI	Original	100 (87.7–100)			
	5.5		100 (87.7–100)	92.9 (76.3–99.1)	0.368
	6.8		92.9 (76.3–99.1)	71.4 (52.8–84.9)	0.002[†‡]
	9.7		7.1 (0.9–23.7)	0 (0–12.3)	< 0.001*[†]
PD	Original	100 (87.7–100)			
	3.2		100 (87.7–100)	92.9 (76.6–99.1)	0.135
	4.0		92.9 (76.6–99.1)	96.4 (81.7–99.9)	0.368
	5.8		82.1 (63.1–93.9)	28.6 (13.2–48.7)	< 0.001[†‡]

When statistically significant differences were demonstrated by post-hoc tests using Bonferroni correction ($p < 0.0167$), symbols (*, [†], [‡]) signify p values between original and CS (*), original and SENSE ([†]), and CS and SENSE ([‡]).
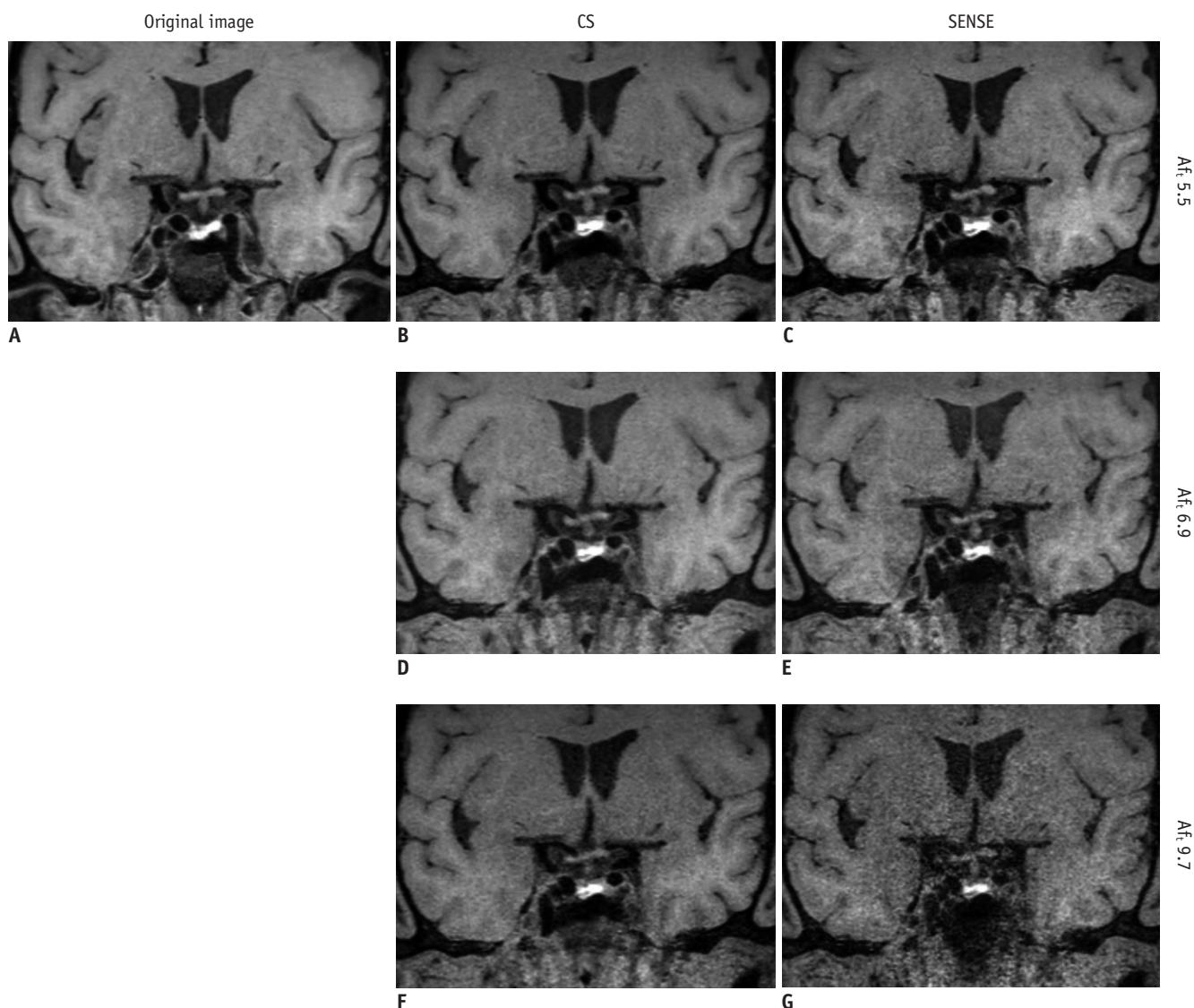
Original image	CS	SENSE

Fig. 3. Reconstructed coronal T1-weighted imaging of 59-year-old man. CS exhibits better image quality and vessel wall delineation than SENSE alone at each AF$_t$. In comparison to original image **(A)**, CS **(B, D, F)** exhibits better image quality and vessel wall delineation than SENSE alone **(C, E, G)** at each AF$_t$. CS **(B)** and SENSE **(C)** images with AF$_t$ 5.5 may be clinically acceptable, whereas SENSE with AF$_t$ 9.7 **(G)** is uninterpretable. AF$_t$ = total acceleration factor, CS = compressed sensing plus SENSE, SENSE = sensitivity encoding

to those of the original sequences ($p > 0.05$) (Table 2). Separate analyses of acceptability for intracranial and extracranial arteries yielded similar results. Representative PD images are shown in Figure 4.

Quantitative Analysis

At AF_t 5.5, 6.8, and 9.7, SNR_{wall} and $CNR_{wall-lumen}$ values on T1WI were significantly higher with CS than with SENSE (p < 0.05). SNR_{lumen} with CS and AF_t 9.7, and SNR_{CSF} with CS and AF_t 6.8 and 9.7 were significantly higher than they were with SENSE ($p < 0.05$). On PD, SNR_{CSF} with CS and AF_t 5.8, and $CNR_{CSF-wall}$ with CS and AF_t 4.0 and 5.8 were significantly higher than they were with SENSE ($p < 0.05$) (Table 3). Separate analyses of intracranial and extracranial arteries yielded similar results (Table 4). At AF_t 5.5 and 9.7, SNR_{wall} values on both intracranial and extracranial T1WI were
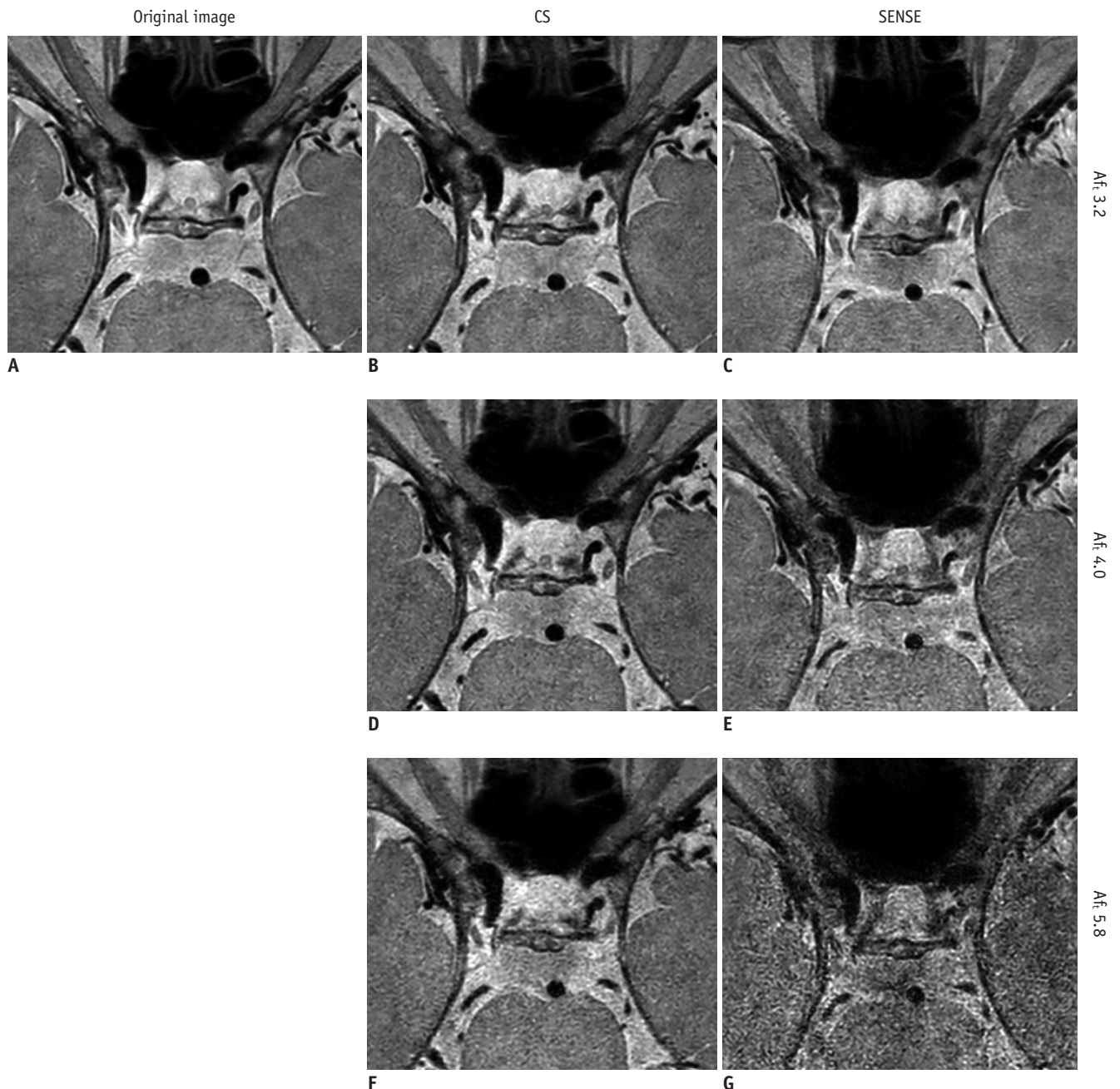
Fig. 4. Axial proton density-weighted imaging of 58-year-old man. CS yielded better image quality and vessel delineation for outer contour and branching arteries than SENSE alone at each AF_t. In comparison to original image **(A)**, CS **(B, D, F)** yielded better image quality and vessel delineation for outer contour and branching arteries than SENSE alone **(C, E, G)** at each AF_t. CS **(B, D)** and SENSE **(C, E)** images with AF_t 3.2 and 4.0 may be clinically acceptable, whereas SENSE with AF_t 5.8 **(G)** is uninterpretable.

Table 3. Comparisons of SNR and CNR between Original, CS, and SENSE Imaging for T1WI and PD HR-MRI

	Acceleration Factor	Original (95% CI)	CS (95% CI)	SENSE (95% CI)	P
T1WI					
SNR_{wall}	Original	12.29 (11.63–12.96)			
	5.5		10.67 (10.07–11.28)	10.06 (9.52–10.61)	< 0.001*†‡
	6.8		8.61 (8.13–9.08)	8.18 (7.75–8.60)	< 0.001*†‡
	9.7		6.56 (6.20–6.92)	5.26 (4.99–5.53)	< 0.001*†‡
SNR_{lumen}	Original	3.35 (3.19–3.52)			
	5.5		2.94 (2.78–3.10)	2.86 (2.71–3.01)	< 0.001*†
	6.8		2.51 (2.39–2.63)	2.55 (2.44–2.66)	< 0.001*†
	9.7		2.16 (2.07–2.26)	1.96 (1.86–2.06)	< 0.001*†‡
SNR_{CSF}	Original	7.51 (7.03–7.99)			
	5.5		6.79 (6.33–7.25)	6.23 (5.63–6.83)	0.002†
	6.8		5.77 (5.39–6.15)	5.26 (4.95–5.57)	< 0.001*†‡
	9.7		4.38 (4.15–4.61)	2.97 (2.80–3.13)	< 0.001*†‡
$CNR_{wall-lumen}$	Original	8.94 (8.32–9.55)			
	5.5		7.73 (7.20–8.26)	7.20 (6.72–7.68)	< 0.001*†‡
	6.8		6.10 (5.65–6.54)	5.63 (5.24–6.01)	< 0.001*†‡
	9.7		4.40 (4.05–4.74)	3.30 (3.06–3.54)	< 0.001*†‡
$CNR_{wall-CSF}$	Original	4.78 (4.15–5.41)			
	5.5		3.95 (3.38–4.53)	3.76 (3.23–4.29)	< 0.001*†
	6.8		2.85 (2.41–3.29)	2.90 (2.46–3.34)	< 0.001*†
	9.7		2.19 (1.88–2.51)	2.29 (1.99–2.58)	< 0.001*†
PD					
SNR_{wall}	Original	3.01 (2.83–3.20)			
	3.2		2.67 (2.50–2.83)	2.48 (2.30–2.66)	< 0.001*†
	4.0		2.34 (2.15–2.53)	2.36 (2.22–2.51)	< 0.001*†
	5.8		2.12 (1.97–2.27)	2.30 (2.16–2.45)	< 0.001*†
SNR_{CSF}	Original	20.51 (19.56–21.47)			
	3.2		16.54 (15.78–17.30)	16.11 (15.23–17.09)	< 0.001*†
	4.0		13.26 (12.58–13.94)	12.39 (11.60–13.17)	< 0.001*†
	5.8		11.34 (10.81–11.87)	8.93 (8.24–9.61)	< 0.001*†‡
$CNR_{CSF-wall}$	Original	17.50 (16.50–18.23)			
	3.2		13.88 (13.48–14.27)	13.63 (13.12–14.14)	< 0.001*†
	4.0		10.92 (10.55–11.29)	10.03 (9.62–10.44)	< 0.001*†‡
	5.8		9.22 (8.96–9.47)	6.62 (6.30–6.94)	< 0.001*†‡

When statistically significant differences were demonstrated by post-hoc tests using Bonferroni correction (Bonferroni corrected p value < 0.05), symbols (*, †, ‡) signify p values between original and CS (*), original and SENSE (†), and CS and SENSE (‡). CNR = contrast-to-noise ratio, CSF = cerebrospinal fluid, SNR = signal-to-noise ratio

significantly higher with CS than with SENSE (p < 0.05). At AF$_t$ 5.5, 6.8, and 9.7, CNR$_{wall-lumen}$ values on intracranial T1WI were significantly higher with CS than with SENSE (p < 0.05). At AF$_t$ 9.7, CNR$_{wall-lumen}$ values on extracranial T1WI were significantly higher with CS than with SENSE (p < 0.05).

Interobserver Agreement

There was good to excellent interobserver agreement between the two observers with regard to the visual scoring system (weighted kappa, 0.784–0.803) and measurements of SNR (ICC, 0.951–0.991) and CNR (ICC, 0.857–0.946).

DISCUSSION

In the current study, HR-MRI of intracranial and extracranial vessels using CS was superior to that using SENSE, yielding higher image quality, better vessel delineation, SNR, and CNR, and a greater proportion of images deemed acceptable. In comparison with the original sequence, CS may be a reliable method for vessel HR-MRI, with comparable image quality and vessel delineation even though T1WI images were acquired in 62% of the original image acquisition time, and PD images were acquired in

Table 4. Comparisons of SNR and CNR between Original, CS, and SENSE Imaging for Intracranial and Extracranial T1WI

	Acceleration Factor	Original (95% CI)	CS (95% CI)	SENSE (95% CI)	P
Intracranial T1WI					
SNR_{wall}	Original	11.58 (10.84–12.31)			
	5.5		9.89 (9.23–10.55)	9.28 (8.70–9.86)	< 0.001*†‡
	6.8		7.87 (7.37–8.37)	7.45 (7.02–7.88)	< 0.001*†
	9.7		6.03 (5.65–6.41)	4.81 (4.53–5.10)	< 0.001*†‡
SNR_{lumen}	Original	3.23 (3.05–3.40)			
	5.5		2.78 (2.62–2.94)	2.73 (2.57–2.88)	< 0.001*†
	6.8		2.49 (2.35–2.63)	2.48 (2.37–2.60)	< 0.001*†
	9.7		2.13 (2.02–2.25)	1.85 (1.75–1.94)	< 0.001*†‡
$CNR_{wall-lumen}$	Original	8.35 (7.68–9.02)			
	5.5		7.11 (6.52–7.69)	6.55 (6.04–7.06)	< 0.001*†‡
	6.8		5.38 (4.92–5.83)	4.97 (4.58–5.36)	< 0.001*†‡
	9.7		3.90 (3.54–4.27)	2.97 (2.71–3.23)	< 0.001*†‡
$CNR_{wall-CSF}$	Original	4.07 (3.37–4.77)			
	5.5		3.14 (2.50–3.78)	3.00 (2.42–3.59)	< 0.001*†
	6.8		2.12 (1.67–2.58)	2.17 (1.71–2.64)	< 0.001*†
	9.7		1.66 (1.34–1.99)	1.84 (1.53–2.16)	< 0.001*†
Extracranial T1WI					
SNR_{wall}	Original	14.44 (13.20–15.68)			
	5.5		13.03 (12.04–14.02)	12.42 (11.55–13.28)	< 0.001†
	6.8		10.83 (10.10–11.56)	10.35 (9.75–10.94)	< 0.001*†
	9.7		8.14 (7.56–8.71)	6.61 (6.26–6.96)	< 0.001*†‡
SNR_{lumen}	Original	3.73 (3.32–4.13)			
	5.5		3.42 (3.03–3.82)	3.25 (2.91–3.60)	< 0.001†
	6.8		2.56 (2.32–2.81)	2.76 (2.47–3.05)	< 0.001*†
	9.7		2.27 (2.08–2.45)	2.31 (2.10–2.51)	< 0.001*†
$CNR_{wall-lumen}$	Original	10.71 (9.46–11.96)			
	5.5		9.60 (8.70–10.51)	9.16 (8.34–9.98)	< 0.001†
	6.8		8.27 (7.58–8.95)	7.59 (6.96–8.21)	< 0.001*†
	9.7		5.87 (5.29–6.45)	4.31 (3.91–4.70)	< 0.001*†‡

When statistically significant differences were demonstrated by post-hoc tests using Bonferroni correction (Bonferroni corrected p value < 0.05), symbols (*, †, ‡) signify p values between original and CS (*), original and SENSE (†), and CS and SENSE (‡).

50% of the original image acquisition time. CS also yielded acceptable T1WI images at AF_t 5.5 and 6.8, and acceptable PD images at AF_t 3.2, 4.0, and 5.8.

Reducing the imaging acquisition time may be crucial for expanding the clinical use of vessel wall HR-MRI in daily practice. Of the various sparse reconstruction techniques available, it has been proposed that CS has promise for intracranial and extracranial vessel wall MRI because it can markedly reduce image acquisition time while preserving image quality. In CS, undersampling of k-space data is achieved via a variable-density random method, which means denser sampling in the central k-space than in the peripheral k-space (17, 18). The sparsity in the k-space data is compensated for by a sparsifying transformation-such as a wavelet transformation-and iterative reconstruction

(17). Differences in the undersampling of k-space data and the specified reconstruction methods may contribute to improved image quality and reduced scanning time compared with conventional parallel imaging. Nonlinear iterative reconstruction has been used to reconstruct magnetic resonance images from fewer phase encodings, thereby resulting in a marked reduction in image acquisition time (7).

A previous study demonstrated that a black-blood fast spin echo sequence with CS facilitated a 37% shorter image acquisition time than conventional T1-weighted sampling perfection with application optimized contrasts using different flip angle evolution, while maintaining comparable image quality for intracranial arteries (9). In the present study, T1WI with CS also yielded image quality

and vessel wall delineation that were comparable to those of original imaging sequences, with an image acquisition time that was 38% shorter (62% of the original scanning time). In another study, CS-based simultaneous 3D black-blood and gray-blood imaging yielded image quality that was comparable to that of a fully sampled acquisition for carotid artery visualization, and achieved it in a shorter scanning time (7). The authors stated that the "signal-to-tissue" and "contrast-to-tissue" ratios did not differ significantly between CS images with AF_t values of 2–5 and original images. In contrast, in the current study SNR and CNR were significantly lower in CS images than in original images, even though image quality and vessel delineation did not differ significantly between them based on results derived from the visual scoring systems. The differences between the results of the two studies may be due to the parameters chosen. The "signal-to-tissue" and "contrast-to-tissue" ratios may reflect the visual assessment more than the quantitative measurements used in the current study (i.e., SNR and CNR).

CS yielded image quality and vessel delineation that were comparable to the original sequences in the present study, with a reduction in image acquisition time of 50% for PD. Vessel HR-MRI generally focused on evaluating arterial walls using T1WI; however, PD imaging with a high SNR also provides useful information on definite vessel contours, detailed vessel anatomy, and small branching arteries (1, 19). Therefore, the use of CS PD sequences for vessel evaluation is worthy of further assessment. To our knowledge, to date no previous study has evaluated CS PD sequences for intracranial vessel HR-MRI.

In the present study, CS T1WI with AF_t 5.5 and 6.8, and SENSE T1WI with AF_t 5.5 yielded respective acceptability rates of 100%, 96.4%, and 100%, while CS PD with AF_t 3.2, 4.0, and 5.8, and SENSE PD with AF_t 3.2 and 4.0 yielded respective acceptability rates of 100%, 92.9%, 82.1%, 92.9%, and 96.4%. At these AF_t values, the proportions of acceptable images did not differ significantly from those of the original imaging. According to results derived via the visual scoring systems, acceptable images could be acquired at higher AF_t values than would otherwise result in image quality comparable to the original sequences. Thus, in terms of clinical acceptability there may be scope to further shorten the acquisition times for both CS and SENSE sequences.

The present study had several limitations. First, it only included 14 healthy volunteers. Further studies including more patients and various clinical applications are required. Second, even the original T1WI and PD sequences included acceleration factors, which may be a limitation with regard to comparisons between original images and CS and SENSE images. Notably however, in clinical practice vessel wall HR-MRI generally includes an acceleration factor to reduce scanning time, and a previous study also compared CS images with original images that included acceleration factors (9). Furthermore, we wished to focus on comparing clinically-used original imaging sequences with CS and SENSE imaging. Third, due to limits on available acquisition time, we only evaluated three different acceleration factors. Further efforts to optimize scanning parameters for CS HR-MRI of vessels are warranted. Fourth, because we only evaluated CS (i.e., compressed sensing combined with SENSE) compared to SENSE alone, it is unclear how the image quality of CS compares with that of compressed sensing alone at the same AF_t factors. Further study is warranted in this respect. Fifth, the study did not generate data for contrast-enhanced T1WI, because the use of gadolinium-based contrast agents is not justified in healthy volunteers.

In conclusion, CS was superior to SENSE with regard to image quality, vessel delineation, SNR, CNR, and acceptability in vessel HR-MRI. CS T1WI with AF_t of 5.5 and CS PD with AF_t of 3.2 and 4.0 may be reliable for HR-MRI of vessels.

Conflicts of Interest

The authors have no financial conflicts of interest.

ORCID

Seung Chai Jung
https://orcid.org/0000-0001-5559-7973
Chong Hyun Suh
https://orcid.org/0000-0002-4737-0530

REFERENCES

1. Mandell DM, Mossa-Basha M, Qiao Y, Hess CP, Hui F, Matouk C, et al.; Vessel Wall Imaging Study Group of the American Society of Neuroradiology. Intracranial vessel wall MRI: principles and expert consensus recommendations of the American Society of Neuroradiology. *AJNR Am J Neuroradiol* 2017;38:218-229

2. Chung MS, Jung SC, Kim SO, Kim HS, Choi CG, Kim SJ, et al. Intracranial artery steno-occlusion: diagnosis by using two-dimensional spatially selective radiofrequency excitation

pulse MR imaging. *Radiology* 2017;284:834-843

3. Lee NJ, Chung MS, Jung SC, Kim HS, Choi CG, Kim SJ, et al. Comparison of high-resolution MR imaging and digital subtraction angiography for the characterization and diagnosis of intracranial artery disease. *AJNR Am J Neuroradiol* 2016;37:2245-2250

4. Park JE, Jung SC, Lee SH, Jeon JY, Lee JY, Kim HS, et al. Comparison of 3D magnetic resonance imaging and digital subtraction angiography for intracranial artery stenosis. *Eur Radiol* 2017;27:4737-4746

5. Saam T, Raya JG, Cyran CC, Bochmann K, Meimarakis G, Dietrich O, et al. High resolution carotid black-blood 3T MR with parallel imaging and dedicated 4-channel surface coils. *J Cardiovasc Magn Reson* 2009;11:41

6. Itskovich VV, Mani V, Mizsei G, Aguinaldo JG, Samber DD, Macaluso F, et al. Parallel and nonparallel simultaneous multislice black-blood double inversion recovery techniques for vessel wall imaging. *J Magn Reson Imaging* 2004;19:459-467

7. Lustig M, Donoho D, Pauly JM. Sparse MRI: the application of compressed sensing for rapid MR imaging. *Magn Reson Med* 2007;58:1182-1195

8. Li B, Li H, Kong H, Dong L, Zhang J, Fang J. Compressed sensing based simultaneous black- and gray-blood carotid vessel wall MR imaging. *Magn Reson Imaging* 2017;38:214-223

9. Zhu C, Tian B, Chen L, Eisenmenger L, Raithel E, Forman C, et al. Accelerated whole brain intracranial vessel wall imaging using black blood fast spin echo with compressed sensing (CS-SPACE). *MAGMA* 2018;31:457-467

10. Fan Z, Yang Q, Deng Z, Li Y, Bi X, Song S, et al. Whole-brain intracranial vessel wall imaging at 3 Tesla using cerebrospinal fluid-attenuated T1-weighted 3D turbo spin echo. *Magn Reson Med* 2017;77:1142-1150

11. Ramesh N, Yoo JH, Sethi IK. Thresholding based on histogram approximation. *IEE P-Vis Image Sign* 1995;142:271-279

12. Raju PDR, Neelima G. Image segmentation by using histogram thresholding. *IJCSET* 2012;2:776-779

13. Qiao Y, Steinman DA, Qin Q, Etesami M, Schär M, Astor BC, et al. Intracranial arterial wall imaging using three-dimensional high isotropic resolution black blood MRI at 3.0 Tesla. *J Magn Reson Imaging* 2011;34:22-30

14. Zhang Z, Fan Z, Carroll TJ, Chung Y, Weale P, Jerecic R, et al. Three-dimensional T2-weighted MRI of the human femoral arterial vessel wall at 3.0 Tesla. *Invest Radiol* 2009;44:619-626

15. Park JE, Han K, Sung YS, Chung MS, Koo HJ, Yoon HM, et al. Selection and reporting of statistical methods to assess reliability of a diagnostic test: conformity to recommended methods in a peer-reviewed journal. *Korean J Radiol* 2017;18:888-897

16. Kang HJ, Lee JM, Joo I, Hur BY, Jeon JH, Jang JY, et al. Assessment of malignant potential in intraductal papillary mucinous neoplasms of the pancreas: comparison between multidetector CT and MR imaging with MR cholangiopancreatography. *Radiology* 2016;279:128-139

17. Yang AC, Kretzler M, Sudarski S, Gulani V, Seiberlich N. Sparse reconstruction techniques in magnetic resonance imaging: methods, applications, and challenges to clinical adoption. *Invest Radiol* 2016;51:349-364

18. Li G, Hennig J, Raithel E, Büchert M, Paul D, Korvink JG, et al. An L1-norm phase constraint for half-Fourier compressed sensing in 3D MR imaging. *MAGMA* 2015;28:459-472

19. Choi YJ, Jung SC, Lee DH. Vessel wall imaging of the intracranial and cervical carotid arteries. *J Stroke* 2015;17:238-255